Jurnal Teknik Mesin
Mechanical Xplore (JTMMX)
Mechanical Engineering
Vol. 4 No. 2 (2024) pp. 47-60
p-ISSN: 2746-0045 e-ISSN: 2746-3672

The Box-Behnken Response Surface Methodology Approach to Optimize Tensile Strength Load in Resistance Spot Welding Using SPCC-SD Steel

Dodi Mulyadi[1*], Amir[1], Ade Cepi Budiyansyah, Sukarman[1,2], Khoirudin[1,2], Ludvi Arif Wibowo[3], Shanti Kumbarasari[4]

[1]Department of Mechanical Engineering, Faculty of Engineering, Universitas Buana Perjuangan Karawang, Jl. HS.Ronggo Waluyo, Karawang, 41361, West Java, Indonesia.

[2]Department of mechanical Engineering, Faculty of Engineering, Universitas Sebelas Maret Jl. Ir. Sutami 36A Kentingan, Surakarta, 5712, Central Java, Indonesia.

[3]Department of Mechanical Engineering, Politeknik Sukabumi, Jl. Babakan Sirna No.25, Sukabumi, 43132, West Java, Indonesia.

[4]Department of Mechanical Engineering, Politenik Industri ATMI Cikarang, Jababeka Education Park, Jl. Raya, Bekasi, J17520, West Java Indonesia.

ABSTRACT

This article describes an experimental investigation into optimizing spot welding resistance (RSW) using a spot-welding machine equipped with a dual-electrode Pressure Force System (PFS). The optimization procedure entails the incorporation of SPCC-SD (JIS G 3141), a low-carbon steel that finds extensive application in the automotive sector. With the widespread use of SPCC-SD steel, RSW is an essential process in the automotive industry for assembling body components. This study employs the Box-Behnken Response Surface Methodology (Box-Behnken-RSM) to optimize the tensile strength load (TS-load), a critical parameter in RSW, through a meticulous analysis of the interplay between Holding Time, Squeezing Time, Welding Current, and Welding Time. Through the methodical design of experiments, the collection of Tensile Strength Load data, and the application of statistical modeling via RSM, this study employs SPCC-SD steel to determine the optimal values for these variables in RSW. The results above readily offer a valuable understanding of the most significant determinants and their interrelationships, thus facilitating advancements in welding methodologies and quality control in the automotive manufacturing sector. This study employs the Box-Behnken Response Surface Methodology to investigate the impacts and interrelationships of different parameters thoroughly. It aims to enhance the TS-load using SPCC-SD steel during the resistance spot welding procedure. This research contributes to advancing welding methodologies employed in the automotive manufacturing sector.

Keywords: *Box-Behnken; Response Surface Methodology; Tensile Strength Load; Resistance Spot Welding*

Article information:
- Submitted: 22/12/2023
- Revised: 26/12/2023
- Accepted: 28/12/2023

Author correspondence:
* ✉:
dodi.mulyadi@ubpkarawang.ac.id

Type of article:

☑ Research papers

☐ Review papers

1. INTRODUCTIONS

The research on resistance spot welding using SPCC-SD steel in automotive body manufacturing is crucial due to its significance as a primary technique in the automotive industry. SPCC-SD steel is frequently utilized in car body manufacturing for its advantages in strength, durability, and ability to be easily shaped according to design needs. The background of this research may involve the development of more efficient joining techniques, enhancement of joint strength, optimization of welding parameters for SPCC-SD steel, investigation of the influence of temperature or pressure variations on the mechanical pro-

https://doi.org/10.36805/jtmmx.v4i2.6090

perties of joints, or even the application of new technologies in resistance spot welding to enhance joint quality in car body structures.

Resistance spot welding (RSW) is a leading welding technology used to assemble car body components in the automotive industry [1, 2]. RSW is the most popular joining method for connecting car body structures in the automotive industry. Each car includes approximately 5,000 spot welds in its assembly process [3-5]. Achieving high efficiency is a significant challenge for researchers and engineers in this field. Welding that fails to meet standards can occur in production due to improper parameters [6].

Resistant spot welding (RSW) stands out by joining metals using high electrical current at specific points, distinguishing it from other welding techniques. In the automotive sector, Resistance Spot Welding (RSW) stands out as the preferred choice for manufacturing car bodies owing to its rapid production and efficiency [7]. Unlike electric arc or gas welding methods, RSW is particularly adept at swiftly and automatically joining thin metals. Laser welding, distinguished by its high precision focus and efficient utilization of laser energy, finds application across a spectrum of heat-sensitive metal types. [8] [9] . Indeed, RSW maintains its position as the primary choice for mass production due to its ability to yield robust, enduring joints while ensuring high efficiency in time. However, the selection of the welding technique relies on the distinct project prerequisites, the thickness of the metal, the type of material being used, and the requisite precision level for the joining process. These factors collectively determine the most suitable method for achieving optimal results in welding. Upon examining the outcomes, disparities between material combinations employing RSW and GTAW/GMAW methods are evident, as illustrated in Figure 1[10].

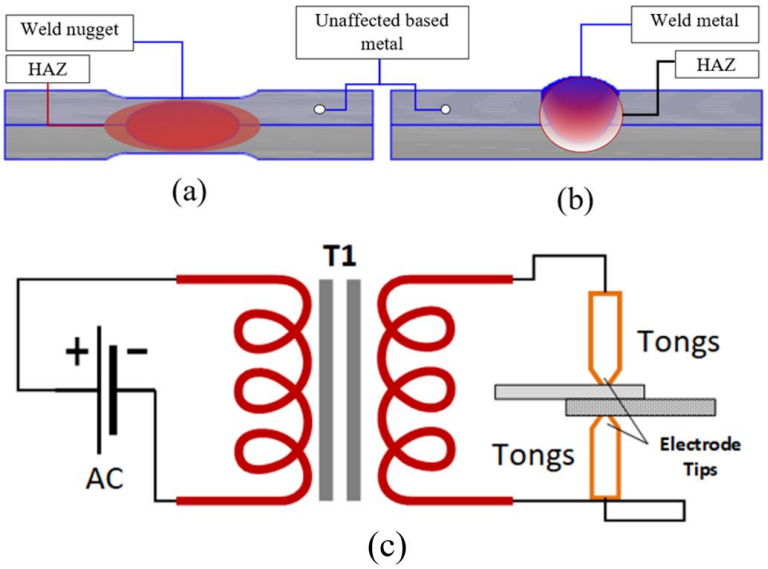

Figure 1. Results of welding comparison: (a) RSW, (b) GMAW, and (c) RSW schematic [10].

Resistance spot welding (RSW) relies on high electrical currents to create the required heat, effectively melting the metal at precise locations between two sheets intended for joining [11]. The procedure entails the placement of electrodes on both sides of the materials to be joined, followed by firmly pressing these metal sheets together [12, 13]. As the electrodes pass a high electrical current, the material's inherent resistance generates heat at the contact points [14, 15]. The produced heat is sufficiently intense to melt the metal at these specific contact areas. With consistent pressure, the molten metal cools and solidifies, forging a robust bond upon the release of the electrodes. The RSW principle relies on controlling electrical currents, applying precise pressure, and employing optimal duration to create robust joints capable of withstanding mechanical loads encountered in car body structures [16, 17]. Metal melting occurs at the metal welding contact due to the heat generated by electrical contact resistance. The fusion process occurs on the surfaces of the adhering metals, which melt due to electrical resistance [18, 19]. The RSW process

occurs during a specific cycle time, where welding current, welding time, and electrode force are crucial process parameters [17, 19]. Electrical resistance also occurs at the electrode contact surface with the plate but does not result in metal melting due to cooling with water at both electrode ends [15].

Metal fusion occurs due to the heat and pressure applied at both ends of the electrodes on the metal surfaces. The pressing process in RSW is provided throughout the welding cycle [17, 20]. The pressing process aims to forge the metal in the nugget area post-heating and prevent deformation (warping) in the joint [15, 21]. In the RSW process, pressing begins in the squeeze time cycle. Welding occurs when the current flows to the electrode end, causing it to heat up and creating fusion between the joined metal surfaces [18, 21]. The latest publications detailing the mechanical properties of welded steel using the RSW technique generally focus exclusively on describing the response of a specific type of steel. Thakur et al. conducted research optimizing RSW parameters for galvanized steel sheets. The study utilized the Taguchi optimization method with parameters including preheating current (kA), squeeze time (cycles), welding current (kA), weld time (cycles), hold time (cycles), and pressure (MPa). ANOVA analysis was employed, with the optimized response parameter being tensile-shear strength. The research confirmed that welding current and time significantly influence tensile-shear strength [22]. Shafee et al. conducted RSW research using low-carbon steel materials with thicknesses of 0.8 and 1.0 mm. The study employed a Taguchi 3-parameter and 3-level experimental method, focusing on electrode force, welding current, and welding time as parameters. Tensile-shear strength and direct-tensile strength were taken as outcomes. S/N ratio analysis using 'higher-is-better' data characteristics revealed that welding current and time affect tensile-shear strength. In contrast, direct-tensile strength is strongly influenced by welding time and welding current [23]. Emre et al. investigated the optimization of RSW for TRIP800 steel using a two-way ANOVA method with welding time and welding current as input parameters. The study employed five levels for welding time and seven for welding current. Two response variables, nugget geometry, and tensile-shear strength, were used. The evaluation results indicated that the nugget diameter and nugget size ratio for TRIP800 steel should be at least $4.5\sqrt{t}$ and 0.15–0.30, respectively. Meeting these two requirements is crucial to achieving the required pull-out failure mode, tensile-shear strength, and the desired surface quality of the nuggets [24]. Vignesh et al. optimized RSW parameters by combining two different materials, namely 316L austenitic stainless steel and 2205 duplex stainless steel. The study employed Taguchi experiments with three parameters and three experimental levels. ANOVA analysis revealed that the significant consecutive influences on tensile-shear strength were welding current, heating cycle, and electrode tip diameter [25].

Applying Response Surface Methodology (RSM) in the resistant spot welding (RSW) process on SPCC-SD steel for car body manufacturing offers an innovative approach to optimizing welding parameters. By utilizing RSM, this study aims to determine parameter combinations (such as current, pressure, and time) that yield optimal joints with high strength and durability in SPCC-SD steel precisely. Through this approach, we anticipate a significant increase in welding process efficiency, reduced product development time, and enhanced structural reliability in car bodies. While previous studies have involved the RSW process on SPCC-SD steel for car body manufacturing, the optimization approach using Response Surface Methodology (RSM) opens new opportunities for process efficiency enhancement. Through the application of RSM, this effort is focused on determining optimal parameters that include welding current (kA), squeeze time (cycles), welding time (cycles), and holding time (cycles), with the primary goal of maximizing the strength and durability of joints in SPCC-SD steel. Consequently, a significant improvement in joint quality, production efficiency, and structural resilience in car bodies is expected, complementing and enhancing previous findings in using RSW on this material.

2. METHOD

2.1. Low Carbon Steel SPCC-SD

The SPCC-SD is a widely utilized steel variant in manufacturing sectors, specifically for the production of automotive components, electronics, and household appliances. The acronym "SPCC" corresponds to the Japanese Standard that defines this particular grade of steel. In this context, "SP" signifies Steel Plate, while "CC" indicates Cold Rolled Coil. SPCC-SD steel is manufactured by subjecting metal to compression at lower temperatures during a cold rolling process, resulting in the formation of steel plates. This steel demonstrates attributes resulting from the cold rolling procedure, including precise dimensional tolerances, sleek surfaces, high strength, and exceptional formability.

SPCC-SD steel is often chosen for its favorable mechanical characteristics, including superior strength, exceptional malleability, and resistance to corrosion after undergoing galvanization. The exceptional qualities of SPCC-SD steel make it extremely adaptable, making it the preferred option in various industrial sectors. Its applications encompass a wide range of fields, such as automotive manufacturing, electronics, household appliances, and precision engineering, due to its dependable performance and versatility in different environments [26]. The chemical composition and materials utilized in this research are presented in Table 1.

Table 1. Mechanical properties and chemical composition of SPCC-SD [13]

Specification	Mechanical properties			Chemical composition (%)			
	Y.P. (N/mm2)	T.S. (N/mm2)	E.L. (%)	C	Mn	P	S
JIS G-3141	Max. 240	Min. 270	Min. 37	Max. 0.15	Max 0.6(	Max 0.04	max 0.05
SP51024*	196	316	43	0.0363	0.193	0.011	0.0051

* Mill Test Certificate

2.2. RSW Machine

This study utilizes a 35 kVA capacity Resistance Spot Welding (RSW) machine for the purpose of conducting welding. The application of pressure to both electrode ends is precisely controlled by a pneumatic mechanism operating at a pressure level of 3.5 MPa. The electrodes are conical in shape, with the diameter of the bottom electrode measuring 8 mm and the diameter of the top electrode measuring 5 mm. The chosen electrode configuration is specifically designed to guarantee accurate contact points on the surfaces of the materials being joined and to maximize the even distribution of heat during the process of RSW [4, 26]. The compressive force at the electrode tip is calculated using Equation (1) [27]:

$$F = P.A \quad (1)$$

Where F represents force (N), P denotes pressure (N/m²), and A is the cross-sectional area (m²). With a top electrode diameter of 5 mm, the compressive force at both electrode ends can be calculated using equation 2, resulting in a pressure of 68.7 N[28].

The RSW metal joining technique commonly experiences two failure modes: pull-out and interfacial. Interfacial failure occurs when the diameter of the molten area at the welding point, known as the 'nugget', is less than the minimum required diameter [29]. Interfacial failure can be attributed to the inadequate welding process, which leads to an imperfect fusion of materials. On the other hand, pull-out failure is considered a foreseeable form of failure in this process. Pull-out failure arises when the joint's strength exceeds that of the base metal. To achieve the desired pull-out failure, it is imperative to ensure that the diameter of the nugget satisfies the minimum requirements stated in a specific equation [19]. The primary objective in the RSW welding process is to achieve a joint that is stronger than the original metal by recognizing and fulfilling these criteria. In order to achieve the pull-out failure model, it is necessary to satisfy the minimum nugget diameter specified in Equation (2) [22, 25, 30].

$$D_{min} = 4.5\sqrt{t} \quad (2)$$

Where t represents the smallest material thickness of the connected metals, as this study employs SPCC-SD material with a thickness of 0.8 mm, the required minimum nugget diameter can be calculated using

equation 3, resulting in a diameter of 4.27 mm. This study utilized electrodes with a diameter of 5.0 mm. The RSW machine used in this research can be seen in Figure 2. This machine plays a crucial role in these experiments, allowing for the accurate application of pressure, current, and time to produce joints that meet the desired specifications. This study aims to achieve maximum results by utilizing an optimized electrode size that meets the previously established requirements for strength and nugget diameter. Figure 2 provides a visual representation of the tool used, playing an integral part in ensuring the success of the experiments and obtaining accurate data for welding result analysis.

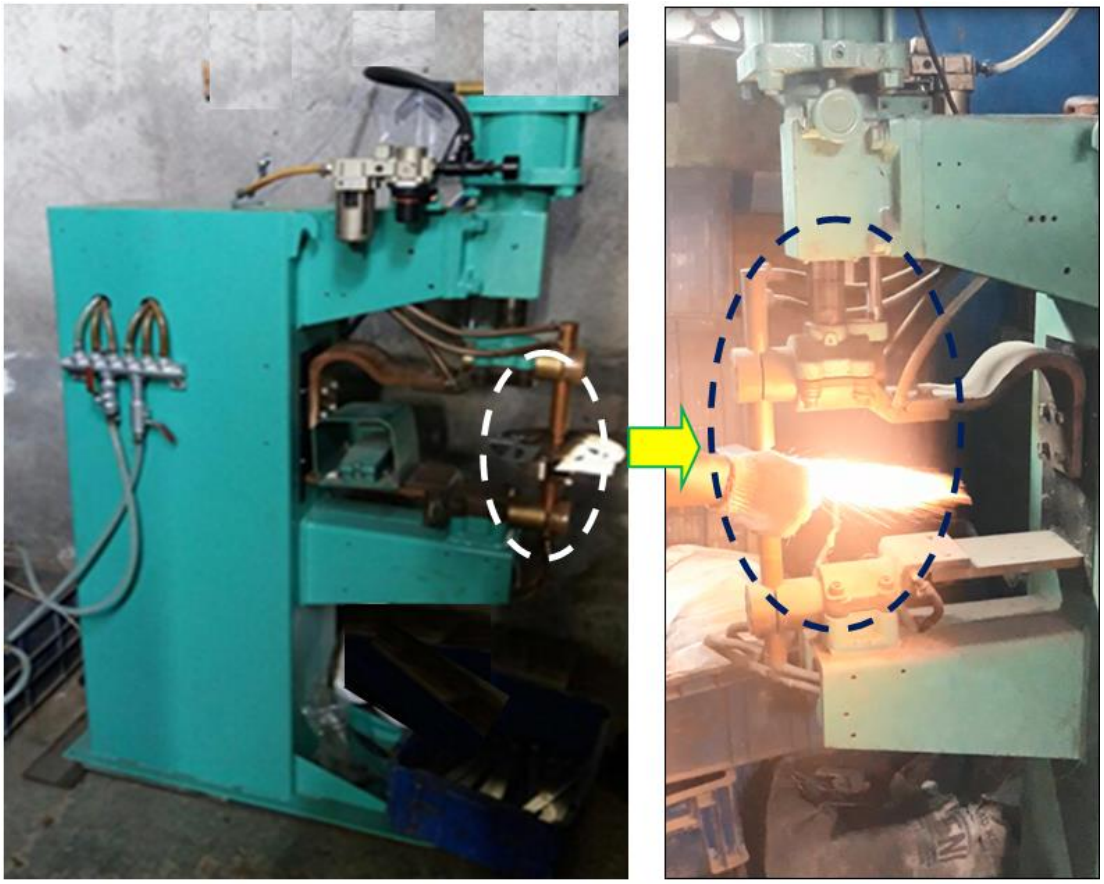

Figure 2. The RSW machine 65kV.

2.3. Box-Behnken Parameter Design

The Box-Behnken parameter design in the context of RSW is an experimental method enabling the testing of system responses to variations in process factors more efficiently [31]. This design employs a geometric box shape to represent multiple levels of each tested process factor, excluding extreme levels that may be impractical or less relevant. The test points are located at both the center and the corners of the box for every factor being tested. This methodology enables the detection of system reactions to changes in the levels of individual factors, without the need to explicitly test all potential combinations. As a result, it optimizes time and resource utilization during the testing phase.

The characteristics of metal joints are profoundly influenced by the management of independent variables such as squeeze time, welding current, holding time, and welding time in RSW. Every parameter fulfills a unique function: the holding time facilitates metal cooling to ensure a robust joint formation, squeeze time controls initial pressure and metal surface contact, and welding current determines the energy supplied to the welding point. Nonetheless, controls over the surface conditions of the base metal and the temperature of the electrode may impose constraints on the quality of the joint. The presence of this variability highlights the importance of developing a deep understanding of the complex relationship

between factors that are under your control and difficult environmental circumstances. Achieving process optimization and ensuring high-quality metal joints requires mastering this interaction. Further information on optimization design using the Box-Behnken experiment design is provided in Table 2.

Table 2. Box-Behnken RSW Parameter Design

Code	*Welding* parameters	Level	
		Low	High
A	Weld. *current* (kA)	18	22
B	Squeeze *time* (*cycles*)	22	27
C	Weld. *time* (second)	0.4	0.6
D	Hold *time* (*cycles*)	12	18

cycle=1/60 second

The summary of the Response Surface Methodology (RSM) in the experimental design reveals that this study conducted 27 fundamental experiments testing four factors or independent variables. These experiments were singular and not repeated, without additional grouping, making each of the 27 trials essential. This design allowed the exploration of various combinations of factor levels to observe the system's response to alterations in the tested process parameters. By implementing RSM in this framework, the study aims to comprehensively understand the interrelation between the investigated factors and the anticipated response within the RSW process [23]. For further details regarding this RSM experimental design, refer to Table 3.

Table 3. Experimental RSM data for TS-load strength

Run	A	B	C	D	TS-load Exp. (N)	TS-load Predict.	Failure mode
1	22	27	0.5	15	5904.35	5777.4	Pull out
2	22	25	0.6	15	5884.05	5712.9	Pull out
3	20	27	0.5	15	5663.66	5468.6	Pull out
4	21	27	0.4	15	5660.01	5583.0	Pull out
5	21	25	0.6	18	5897.52	5557.3	Pull out
6	21	27	0.5	12	5650.19	5624.2	Pull out
7	21	22	0.4	15	4853.35	5374.0	Pull out
8	20	25	0.5	18	5374.52	5362.9	Pull out
9	21	27	0.6	15	5938.12	5663.0	Pull out
10	22	25	0.4	15	5406.67	5632.9	Pull out
11	22	25	0.5	12	5563.09	5674.1	Pull out
12	21	27	0.5	18	5805.93	5621.8	Pull out
13	22	25	0.5	18	5631.07	5671.7	Pull out
14	21	25	0.4	18	5246.08	5477.3	Pull out
15	20	25	0.4	15	5103.81	5324.1	Pull out
16	21	25	0.6	12	5741.78	5559.7	Pull out
17	20	22	0.5	15	5492.63	5259.6	Pull out
18	21	22	0.5	12	5104.75	5415.2	Pull out
19	21	25	0.5	15	5459.03	5518.5	Pull out
20	20	25	0.6	15	5755.25	5404.1	Pull out
21	21	22	0.6	15	5601.05	5454.0	Pull out
22	22	22	0.5	15	5283.60	5568.4	Pull out
23	21	22	0.5	18	5095.53	5412.8	Pull out
24	20	25	0.5	12	5242.40	5365.3	Pull out
25	21	25	0.4	12	5166.72	5479.7	Pull out
26	21	25	0.5	15	5459.03	5518.5	Pull out
27	21	25	0.5	15	5459.03	5518.5	Pull out

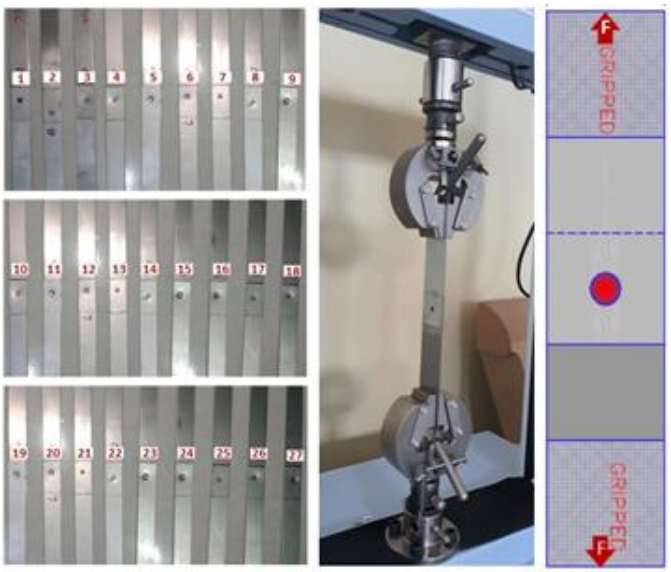

Figure 3. TS coupon and testing process

Surface plots on TS-load are a data visualization method used in data analysis to comprehend how combinations of two independent variables affect the response of TS-load in an experiment [32]. In a surface plot, the x and y axes represent the two independent variables being tested, such as squeeze time (pressure cycles), welding current, welding time, and holding time. Meanwhile, the z-axis represents the TS-load response. This plot displays a three-dimensional surface illustrating the relationship between the independent variables and the observed response [30]. This surface can take on undulating, curving, or flat shapes, reflecting the relationship between the independent variables and the measured response.

Through surface plots, it becomes evident how combining two independent variables collectively influences TS-load. Changes in one independent variable at a specific point on the surface plot will indicate how the TS-load response changes concerning the other independent variable. It aids in a better understanding of the interaction between independent variables and how their combinations can affect the desired response in metal welding, especially in the case of TS-load.

2.4. Statistical Probability Plot

The statistical probability plot is a visualization approach used to examine the distribution of a dataset. This plot aids in evaluating whether the data adheres to a specific distribution, such as a normal distribution or any other [33]. This plot arranges data from smallest to largest and then plots against its probability. If the data adheres to a certain distribution, the plot will display a straight-line pattern or a curve corresponding to the expected distribution. It helps assess the data's fit to a specific statistical model. ANOVA is utilized to compare the means of three or more different groups to determine whether these groups have significant differences [34, 35]. ANOVA measures the variance within each group and compares it with the group variability. If the difference between the means of these groups is significant compared to the variability within the groups, ANOVA will indicate significant differences among the groups. These methods will be employed in statistical analysis to assess data distribution and compare the means of multiple groups aiding in decision-making and data interpretation within the context of statistical research or experimentation.

3. RESULT AND DISCUSIONS

3.1. Tensile-shear Load (TS-load) Analysis

Figure 4 illustrates that the ninth iteration demonstrates the most excellent TS-load, measuring

5938.12 N. The observed value deviates by around 10% from the value predicted by Equation 3. This condition was attained by combining the following parameters—21 time kA for welding current, 27 cycles for squeeze, 0.6 seconds for welding time, and 15 for holding time. During the seventh iteration, the tensile-shear strength is recorded as its minimum value of 4853.35 N. The condition above was attained through a parameter combination consisting of 21 kA for welding current, 21 cycles for holding time, and 0.4 seconds for welding time. The graph illustrating the TS-loads test is provided in Figure 4.

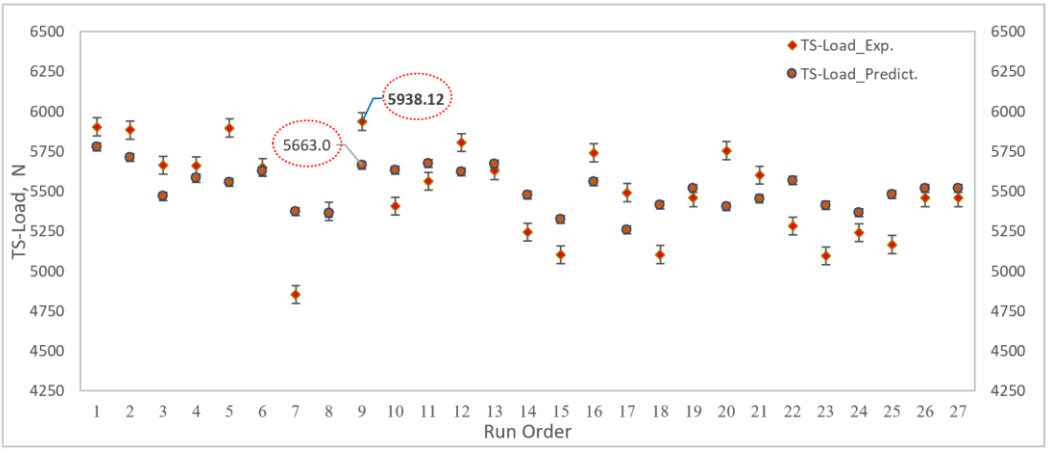

Figure 4. TS-Load experiment and predictions

The TS-loads of all tested samples welded using the RSW technique on SPCC-SD metal showed the expected pull-out failure mode. It contrasts with the tests conducted by [36], where specific processes experienced interfacial failure using a welding time of 0.4 cycles. It suggests that all fusion processes during the RSW process between SPCC-SD metals took place smoothly and without interruption. This phenomenon is explicable by the lack of a zinc layer on the surface of SPCC-SD steel, as shown in [10, 34]. In contrast to the RSW process reported by [10, 37] of the RSW process, the amalgamation of specific parameters demonstrated satisfactory efficacy in the fusion of SPCC-SD steel. Figure 5 presents the results that show the highest TS-load.

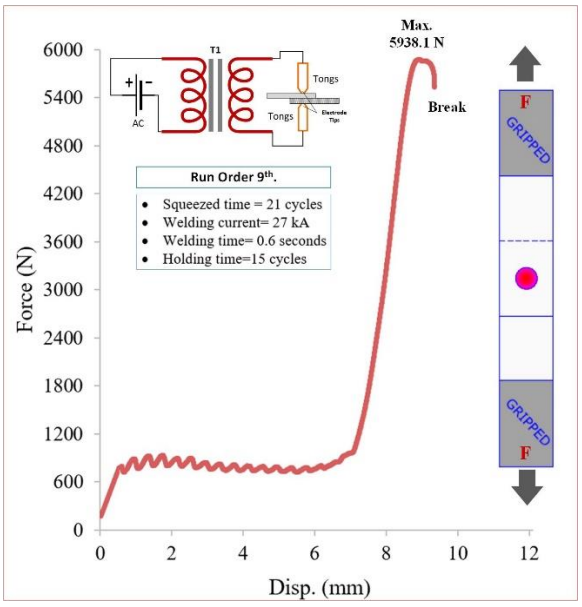

Figure 5. The highest TS-load achieved when joining SPCC-SD steel using the RSW-RSM methods

The TS-load is greater for the highest RSW test results than the initial results documented in [15, 23, 38]. The maximum TS-load values depicted in Figure 4 are approximately 5938.12 N. This result is

approximately 1359.9 N greater than reported in [15]. Compared to the findings documented in references [23] and [38], the results obtained in the present study exhibit an increase of 1279 N and 1179 N, respectively. However, compared to the findings of the study conducted by [18], these results remain somewhat lower at approximately 7354 N. It is explicable given that the tensile strength of manganese steel, utilized in the study reported in [18]], is 2.2 times that of SPCC-SD steel. These results demonstrate that the RSW results can be strengthened by employing the appropriate parameters. In addition, the material's tensile strength impacts the TS-load test value during the RSW process.

3.2. The Contour Plot and Surface Plot Analysis

The contour plots enable the visualization of zones where specific combinations of these parameters yield particular outcomes in metal RSW joints. The contour plot analysis of RSW process on SPCC-SD steel offers a comprehensive depiction of the distribution of heat and mechanical properties at the welding location. Figure 6 exhibits contour plots (i) and surface plots (ii) representing key process parameters, including A: welding current (in kA), B: squeeze time (in cycles), C: welding time (in seconds), and D: hold time (in cycles). The regions are characterized by consistent heat dispersion, corresponding to variations in process variables such as welding current or welding time. In Figure 6 (a), the contour plot and surface plot illustrate the correlation between the TS-load and parameters A and B, with constant conditions of 24.5 cycles for C and 0.4 seconds for D. This visualization provides essential insights into comprehending the TS-load within the domain of RSW. As shown in Figure 6 (b), the contour plot and surface plot show how the TS-load is related to parameters B and D, with B staying at 24.5 cycle and D cycling 15.5 times. Both the contour plot and the surface plot in Figure 6 (c) show how the TS-load is related to parameters A and D, with B always being 24.5 cycle and C always being 0.5 seconds. As shown in Figure 6 (d), the contour plot and surface plot show how the TS-load is related to parameters B and C, with 21 kA for A and 16.5 cycles for D staying the same. Figure 6 (e) illustrates the correlation between the TS-load and parameters B and D, maintaining constant conditions of 21 kA for A and 0.5 seconds for C. Figure 6 (f) reveals the correlation between the TS-load and parameters C and D, maintaining constant conditions of 21 cycles for A and 24.5 cycle for B. This allows for process parameter adjustments to improve the welding quality of SPCC-SD steel. Examining contour plots about RSW process parameters is crucial for comprehending and enhancing the welding process for this material.

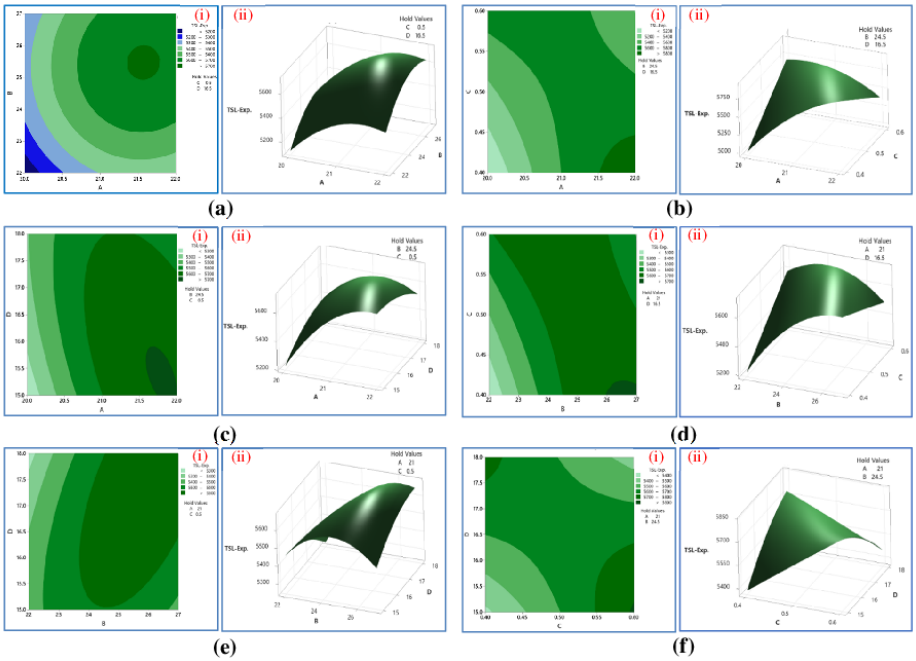

Figure 6. The contour plot of TS-load results.

3.3. ANOVA Evaluations

An ANOVA analysis determines the input parameter with the greatest impact on the response variable (TS-load). This study employs four parameters, specifically A= Weld. The current is represented by the variable B, the squeeze time is represented by the variable C, and the weld time is represented by the variable D. The ANOVA evaluation was conducted using linear, quadratic, and two-way interaction models as listed in Table 4.

The linear ANOVA analysis revealed that the welding current parameter, denoted as A, had the highest influence on the TS-load value, accounting for approximately 66% of the variation. The ANOVA square modeling revealed that the parameters A*A (welding current squared) and B*B (squeeze time squared) were the primary factors influencing the TS-load value, contributing approximately 47% and 48%, respectively. Additionally, the 2-Way Interaction ANOVA is being conducted. The modeling analysis revealed that the parameters A*C, representing the welding current multiplied by the weld time, are the primary factors influencing the TS-load value, contributing approximately 57% to its variation. The findings of this analysis indicate that the TS-load on RSW is significantly affected by the welding current and Weld Time parameters. It validates the findings presented by [2, 16, 25] that these two factors have the greatest impact on the quality of RSW.

Table 4. ANOVA with linear, square and 2-way interactions modeling

Model	Parameter Input	DF	Adj SS	Adj MS	F-Value	P-Value	% Contributions
Linear	A	1	285970	285970	3.69	0.079	66%
	B	1	125974	125974	1.63	0.226	29%
	C	1	19207	19207	0.25	0.627	4%
	D	1	4	4	0	0.994	0%
Model	**Parameter Input**	**DF**	**Adj SS**	**Adj MS**	**F-Value**	**P-Value**	**% Contributions**
Square	A*A	1	102796	102796	1.33	0.272	47%
	B*B	1	103595	103595	1.34	0.27	48%
	C*C	1	23	23	0	0.987	0%
	D*D	1	11250	11250	0.15	0.71	5%
Model	Parameter Input	DF	Adj SS	Adj MS	F-Value	P-Value	**% Contributions**
2-Way Interaction	A*B	1	347	347	0	0.948	0%
	A*C	1	371706	371706	4.8	0.049	57%
	A*D	1	30181	30181	0.39	0.544	5%
	B*C	1	89831	89831	1.16	0.303	14%
	B*D	1	35259	35259	0.46	0.513	5%
	C*D	1	125145	125145	1.62	0.228	19%

3.4. The Probability Plot Analysis

The normal probability plot illustrates the comparison between the sample means of TS-Load values and the expected means, assuming a normal distribution [30]. If the points on the plot exhibit a linear pattern, it indicates that the data provided follows a normal distribution [39]. Deviations from the norm could potentially be inferred from any deviation from a straight line [40]. A normal probability plot is displayed in Figure 7, which compares the sample means of TS-Load values acquired from RSW. The purpose of this plot is to examine and compare the mean distribution of the data points in question with the expected theoretical values predicted by a normal distribution. The utilization of these visual representations is essential when evaluating the data's conformity to a normal distribution and detecting any anomalies or recurring trends in the means of the TS-Load values.

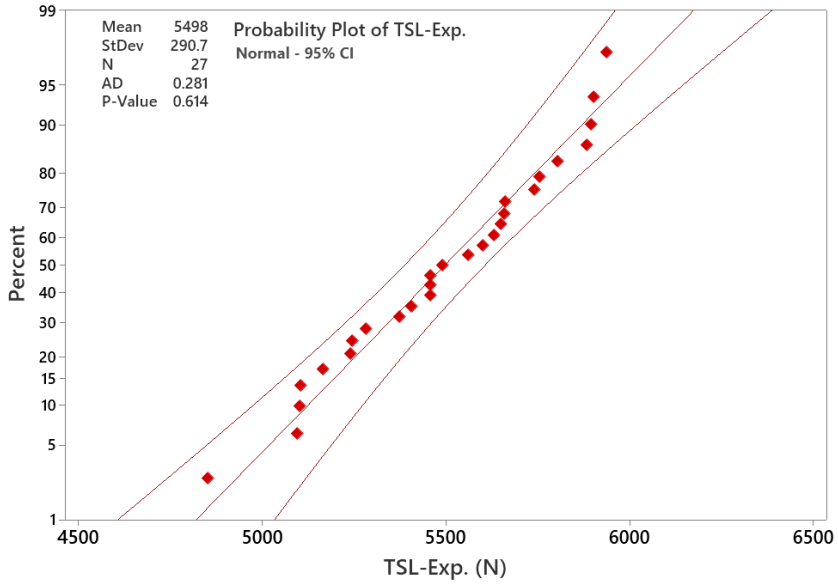

Figure 7. Probability plot of TS-load

The data presented in Figure 7 indicates that the mean value of the 27 samples is approximately 5498 N, with a standard deviation of 290.7 N, representing approximately 5.3% of the mean value. A confidence level of 95% accompanies the provided information. The examination of the data reveals that the precision of every TS-load result is maintained within the range of 5%.

Furthermore, it is worth noting that the data reveals that a TS-load value of 4853.35 N occurred exclusively at the seventh iteration, which is below 5000 N. Furthermore, based on the data observations, it can be inferred that the TS-load value has already attained an approximate 50% level of achievement prior to reaching the mean condition. This enhancement signifies a more favorable result than the study documented in the citation [28].

4. CONCLUTIONS

The utilization of SPCC-SD metal in conjunction with the RSW technique was executed by adjusting the RSW parameters and applying a compressive force of 68.7 N. Current and welding time are crucial variables that significantly impact the attainment of the maximum TS-load. The maximum values for the weld current and holding time were ascertained to be 22 kA, 27 cycles of squeeze, 0.6 seconds of welding, and 15 cycles, respectively, which led to the attainment of TS-load output in the ninth iteration. In the interim, the minimum values for the TS-load output achieved in the seventh iteration were identified: a welding current of 21 kA, a squeeze time of 22 cycles, a welding time of 0.4 seconds, and a holding time of 15 cycles. It can significantly prevent interface failure modes by controlling the welding current and time parameters. In light of these two phenomena, however, RSW welding techniques employing the RSM methodology advise against using the seventh parameter. The following recommendation pertains to using the RSW technique for SPCC-SD metal amalgamation: welding time parameters falling below 0.4 seconds are not advised. Future research will examine the impact of electrode diameter on nugget diameter and tensile shear strength.

AUTHOR'S DECLARATION

Authors' contributions and responsibilities

The authors made substantial contributions to the conception and design of the study. The authors took responsibility for data analysis, interpretation and discussion of results. The authors read and approved the final manuscript.

Acknowledgment

The author would like to thank all the teams involved in this research. The authors also thank the laboratory staff at the manufacture, The University of Buana Perjuangan Karawang laboratory. The author would also like to thank the PT Isaka Alindo Nusantara team for providing input and allowing us to use the RSW machine.

Availability of data and materials

All data are available from the authors.

Competing interests

The authors declare no competing interest.

REFERENCES

[1] S. T. Pasaribu, S. Sukarman, A. D. Shieddieque, and A. Abdulah, "Optimasi Parameter Proses Resistance Spot Welding pada Pengabungan Beda Material SPCC."

[2] A. G. Thakur and V. M. Nandedkar, "Optimization of the Resistance Spot Welding Process of Galvanized Steel Sheet Using the Taguchi Method," *Arabian Journal for Science and Engineering*, vol. 39, no. 2, pp. 1171-1176, 2014.

[3] H. Miller, *Handbook for Resistance Spot Welding*. Miller Electric Mfg. Co., 2010.

[4] M. Tumuluru, *Resistance spot weld performance and weld failure modes for dual phase and TRIP steels*. Woodhead Publishing Limited, 2010, pp. 43-64.

[5] Y. G. Kim, D. C. Kim, and S. M. Joo, "Evaluation of tensile shear strength for dissimilar spot welds of Al-Si-Mg aluminum alloy and galvanized steel by delta-spot welding process," *Journal of Mechanical Science and Technology*, vol. 33, no. 11, pp. 5399-5405, 2019.

[6] Y. B. Li, Q. X. Zhang, L. Qi, and S. A. David, "Improving austenitic stainless steel resistance spot weld quality using external magnetic field," *Science and Technology of Welding and Joining*, vol. 23, no. 7, pp. 619-627, 2018.

[7] S. Sukarman and A. Abdulah, "Optimasi parameter resistance spot welding pada pengabungan baja electro-galvanized menggunakan metode Taguchi," *Dinamika Teknik Mesin*, vol. 11, no. 1, pp. 39-48, 2021.

[8] N. Den Uijl, F. Azakane, S. Kilic, and V. Docter, "Performance of tensile tested resistance spot and laser welded joints at various angles," *Welding in the World*, vol. 56, no. 11-12, pp. 143-152, 2012.

[9] V. Gautam and D. R. Kumar, "Experimental and numerical investigations on springback in V-bending of tailor-welded blanks of interstitial free steel," *Proceedings of the Institution of Mechanical Engineers, Part B: Journal of Engineering Manufacture*, vol. 232, no. 12, pp. 2178-2191, 2018.

[10] F. Mucharom *et al.*, "Tensile shear load in resistance spot welding of dissimilar metals: An optimization study using response surface methodology," *Mechanical Engineering for Society and Industry*, vol. 3, no. 2, pp. 66-77, 2023.

[11] W. Wang, M. Hua, and X. Wei, "A comparison study of sliding friction behavior between two high strength DP590 steel sheets against heat treated DC53 punch: Hot-dip galvanized sheet versus cold rolled bare sheet," *Tribology International*, vol. 54, pp. 114-122, 2012.

[12] K. Nagatsuka *et al.*, "Dissimilar materials joining of metal/carbon fibre reinforced plastic by resistance spot welding," *Welding International*, vol. 32, no. 7, pp. 505-512, 2018.

[13] P. Muthu, "Optimization of the Process Parameters of Resistance Spot Welding of AISI 316l Sheets Using Taguchi Method," *Mechanics and Mechanical Engineering*, vol. 23, no. 1, pp. 64-

69, 2019.
[14] Y. Jia, G. Chi, W. Li, Z. Wang, and L. Cui, "Influence of wear pattern of graphite electrode on EDM geometric accuracy of slot machining," *Procedia CIRP*, vol. 95, pp. 408-413, 2020.
[15] D. Ren, D. Zhao, L. Liu, and K. Zhao, "Clinch-resistance spot welding of galvanized mild steel to 5083 Al alloy," *International Journal of Advanced Manufacturing Technology*, vol. 101, no. 1-4, pp. 511-521, 2019.
[16] N. K. Singh and Y. Vijayakumar, "Application of Taguchi method for optimization of resistance spot welding of austenitic stainless steel AISI 301L," *Innovative Systems Design and Engineering*, vol. 3, no. 10, pp. 49-61, 2012.
[17] T. Jagadeesha, "Experimental studies in weld nugget strength of resistance spot-welded 316L austenitic stainless steel sheet," *International Journal of Advanced Manufacturing Technology*, vol. 93, no. 1-4, pp. 505-513, 2017.
[18] R. Ribeiro, E. L. Romão, S. Costa, E. Luz, and J. H. Gomes, "Optimization of the resistance spot welding process of 22MnB5-galvannealed steel using response surface methodology and global criterion method based on principal components analysis," *Metals*, vol. 10, no. 10, pp. 1-25, 2020.
[19] B. Xing, Y. Xiao, Q. H. Qin, and H. Cui, "Quality assessment of resistance spot welding process based on dynamic resistance signal and random forest based," *International Journal of Advanced Manufacturing Technology*, vol. 94, no. 1-4, pp. 327-339, 2018.
[20] Y. Xie, Y. Cai, X. Zhang, and Z. Luo, "Characterization of keyhole gas tungsten arc welded AISI 430 steel and joint performance optimization," *International Journal of Advanced Manufacturing Technology*, vol. 99, no. 1-4, pp. 347-361, 2018.
[21] J. Y. Cheon *et al.*, "Optimization of pulsed current in resistance spot welding of Zn-coated hot-stamped boron steels," *Journal of Mechanical Science and Technology*, vol. 33, no. 4, pp. 1615-1621, 2019.
[22] A. G. Thakur, T. E. Rao, M. S. Mukhedkar, and V. M. Nanedkar, "Application of Taguchi Method for Resistance Spot Welding of Galvanized Steel," vol. 5, no. 11, 2010.
[23] S. Shafee, B. B. Naik, and K. Sammaiah, "Resistance Spot Weld Quality Characteristics Improvement By Taguchi Method," *Materials Today: Proceedings*, vol. 2, no. 4-5, pp. 2595-2604, 2015.
[24] H. E. Emre and R. Kaçar, "Development of weld lobe for resistance spot-welded TRIP800 steel and evaluation of fracture mode of its weldment," *International Journal of Advanced Manufacturing Technology, Springer*, vol. 85, pp. 1737-1747, 2016.
[25] K. Vignesh, A. E. Perumal, and P. Velmurugan, "Optimization of resistance spot welding process parameters andmicrostructural examination for dissimilar welding of AISI 316L austenitic stainless steel and 2205 duplex stainless steel," *International Journal of Advanced Manufacturing Technology*, pp. 455-465, 2017.
[26] M. K. Wahid, M. N. Muhammed Sufian, and M. S. Firdaus Hussin, "Effect of fatigue test on spot welded structural joint," *Jurnal Teknologi*, vol. 79, no. 5-2, pp. 95-99, 2017.
[27] C. Miller Electric Mfg, "Handbook for Resistance Spot Welding," 2012.
[28] X. Wan, Y. Wang, and D. Zhao, "Multi-response optimization in small scale resistance spot welding of titanium alloy by principal component analysis and genetic algorithm," *International Journal of Advanced Manufacturing Technology*, vol. 83, no. 1-4, pp. 545-559, 2016.
[29] S. K. Khanna, C. He, and H. N. Agrawal, "Residual stress measurement in spot welds and the effect of fatigue loading on redistribution of stresses using high sensitivity Moiré interferometry," *Journal of Engineering Materials and Technology, Transactions of the ASME*, vol. 123, no. 1, pp. 132-138, 2001.
[30] F. A. Ghazali *et al.*, *Three Response Optimization of Spot-Welded Joint Using Taguchi Design and*

Response Surface Methodology Techniques. Springer Singapore, 2019, pp. 85-95.

[31] T. Sultan, A. Kumar, and R. D. Gupta, "Material Removal Rate, Electrode Wear Rate, and Surface Roughness Evaluation in Die Sinking EDM with Hollow Tool through Response Surface Methodology," *International Journal of Manufacturing Engineering*, vol. 2014, pp. 1-16, 2014.

[32] L. Selvarajan, M. Manohar, A. Udhaya kumar, and P. Dhinakaran, "Modelling and experimental investigation of process parameters in EDM of Si3N4-TiN composites using GRA-RSM," *Journal of Mechanical Science and Technology*, vol. 31, no. 1, pp. 111-122, 2017.

[33] Minitab. (2023, 10/12/2023). *Overview for Probability Plot*.

[34] S. Sukarman, A. Abdulah, A. D. Shieddieque, N. Rahdiana, and K. Khoirudin, "OPTIMIZATION OF THE RESISTANCE SPOT WELDING PROCESS OF SECC-AF AND SGCC GALVANIZED STEEL SHEET USING THE TAGUCHI METHOD," *SINERGI*, vol. 25, no. 3, pp. 319-328, 2021.

[35] S. Sukarman, A. D. Shieddieque, C. Anwar, N. Rahdiana, and A. I. Ramadhan, "Optimization of Powder Coating Process Parameters in Mild Steel (Spcc-Sd) To Improve Dry Film Thickness," *Journal of Applied Engineering Science*, vol. 19, no. 2, pp. 1-9, 2021.

[36] S. Sukarman *et al.*, "Optimization of Tensile-Shear Strength in the Dissimilar Joint of Zn-Coated Steel and Low Carbon Steel," *Automotive Experiences*, vol. 3, no. 3, pp. 115-125, 2020.

[37] S. Sukarman, A. Abdulah, D. A. Rajab, and C. Anwar, "Optimization of Tensile-Shear Strength in the Dissimilar Joint of Zn-Coated Steel and Low Carbon Steel," *Automotive Experiences*, vol. 3, no. 3, pp. 115-125, 2020.

[38] E. Gunawan, S. Sukarman, A. D. Shieddieque, and C. Anwar, "Optimasi Parameter Proses Resistance Spot Welding pada Pengabungan Material SECC-AF," no. September, 2019.

[39] J. Liu, G. Xu, X. Gu, and G. Zhou, "Ultrasonic test of resistance spot welds based on wavelet package analysis," *Ultrasonics*, vol. 56, pp. 557-565, 2015.

[40] P. G. Mathews, *Design of Experiments with MINITAB*, 12 ed. Milwaukee: Mathews, Paul G., 2005, pp. 205-205.